NJC

ROYAL SOCIETY OF CHEMISTRY

PAPER

View Article Online
View Journal

Cite this: DOI: 10.1039/d5nj03387j

Boric/boronic acid-promoted redox transformation of 4-hydroxy-1,2,3,4-tetrahydroacridine *N*-oxides to functionalized 2,3-dihydroacridin-4(1*H*)-ones and mechanistic studies using DFT calculations

Subir Majhi, Thangellapally Shirisha, Suman Das, Mohmmad Faizan, Ravinder Pawar * and Dhurke Kashinath *

Received 22nd August 2025,
Accepted 30th November 2025

DOI: 10.1039/d5nj03387j

rsc.li/njc

Herein, we have demonstrated the dual functionality of boric and/or boronic acids as reducing agents in the reduction of 1,2,3,4-tetrahydroacridine *N*-oxides into azaaromatics and as oxidizing agents in the oxidation of benzylic alcohols (C(sp^3)–OH) at the C4 position of 4-hydroxy-1,2,3,4-tetrahydroacridine *N*-oxides into the corresponding ketones, furnishing a series of 2,3-dihydroacridin-4(1*H*)-one derivatives. The 4-hydroxy-1,2,3,4-tetrahydroacridine *N*-oxide precursors are synthesized *via* a Cu-catalysed, regioselective C(sp^3)–H hydroxylation of tetrahydroacridine *N*-oxides under aerobic conditions. This protocol exhibits broad substrate scope and high selectivity, affording dihydroacridinones in excellent yields under mild conditions. The integration of experimental data with density functional theory (DFT) calculations provides valuable insights into the intricate reaction mechanism, shedding light on the dual-reaction pathways facilitated by boric/boronic acids.

Introduction

Nitrogen heterocycles are unequivocally privileged scaffolds in medicinal chemistry, playing an indispensable role in drug discovery and pharmaceutical development, which necessitates continuous advancements in their efficient synthesis and structural diversification to access novel therapeutic agents.[1] Among those, acridine and tetrahydroacridine derivatives are nitrogen-containing heterocyclic compounds that have attracted great attention due to their unique physical and chemical properties, with a broad spectrum of biological properties, such as anticancer, antimalarial, antiviral, anti-inflammatory, antitubercular, antimicrobial, antiparasitic, and fungicidal activities (Fig. 1).[2] Beyond their therapeutic potential, these compounds are also effective as acetylcholinesterase inhibitors for the treatment of Alzheimer's disease and find utility in materials science as potential organic electronic device and organic light-emitting diode materials.[3,4] A key functionality that often enhances the biomedical utility of such molecules is the *N*-oxide group. *N*-Oxides are prevalent in nature and play a crucial role in medicinal chemistry as synthetic intermediates, prodrugs, and active drugs (Fig. 1).[5] This functionality can enhance water solubility, decrease membrane permeability, or impact redox reactivity, which is vital for drug targeting and cytotoxicity.

Meanwhile, organoboron reagents are ubiquitous in organic chemistry due to their broad application in cross-coupling

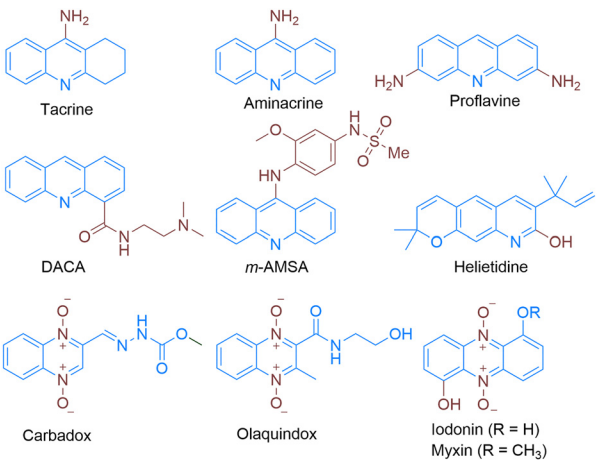

Fig. 1 Synthetic and natural bioactive derivatives of tetrahydroacridine/acridines and related heterocyclic *N*-oxides.

Department of Chemistry, National Institute of Technology, Warangal, 506 004, India. E-mail: ravinder_pawar@nitw.ac.in, kashinath@nitw.ac.in, kashinath.dhurke@gmail.com; Tel: +91-870-2462677

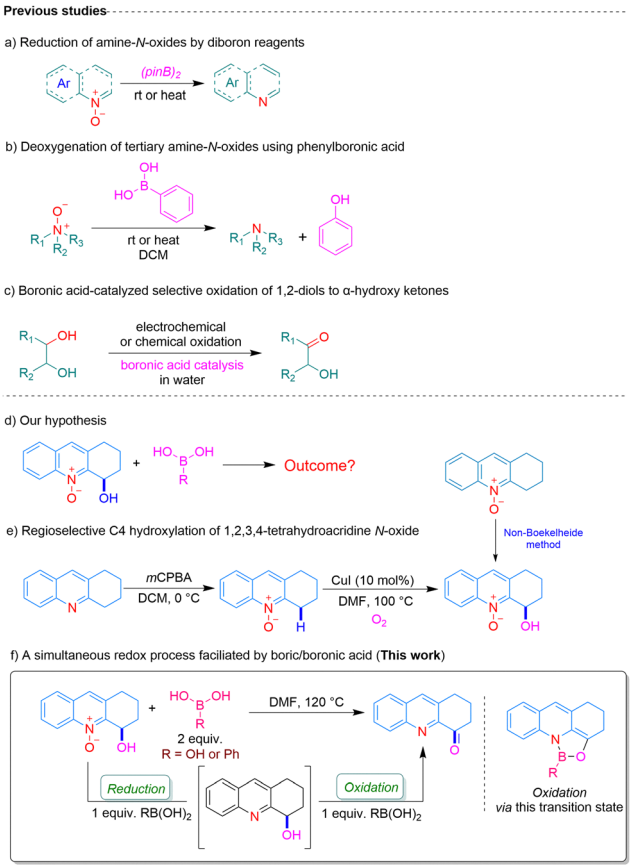

Fig. 2 Synthetic applications of boric/boronic acids and present work for the redox reaction.

chemistry.[6] Beyond their established function as synthetic reagents, boronic acids and other organoborane species exhibit remarkable catalytic activity attributable to the distinctive electronic characteristics of boron atoms.[7] In this context, Hall and Taylor's research groups have published scholarly reviews on organoboron acids as catalysts.[8,9] The Lewis acid nature of organoboron species makes them more promising reagents for catalysis, which generally relies on the complexation of the substrate to boron as a Lewis acid–base complex.[10] Thus, several general reactions become popular targets for organoboron catalysis, like alkylation, carbonyl condensation, cycloaddition, acylation, and dehydration.[10,11] Contrary to the typical function of organoborons, Kokatla *et al.* found bis(pinacolato)diboron to be an excellent reducing agent for aliphatic, aromatic, and heteroaromatic *N*-oxides (Fig. 2a).[12a] Building upon this, numerous strategies have since been developed to achieve *N*-oxide reduction using various boron derivatives.[12b–d] Later, phenylboronic acid was also explored as a reducing agent for the reduction of tertiary amine *N*-oxides (Fig. 2b).[13] Additionally, the metal-free reduction of phosphine oxides, sulfoxides, and *N*-oxides was achieved with hydrosilanes, where borinic acid was used as a precatalyst.[14] Later, boric acid-catalyzed amidation and boronate-ester-catalyzed amide bond formation were also reported.[15] Apart from the catalytic activity and reducing nature of boron species, a couple of oxidation reaction processes were also known, such as the chemoselective oxidation of sulphides to sulfoxides or sulfones and conversion of 1,2-diols to α-hydroxy ketones using boric acid as a catalyst (Fig. 2c).[16] Motivated by the dual reactivity of boron and the biological significance of 1,2,3,4-tetrahydroacridine, we envisioned a redox-active substrate bearing both reducible (*N*-oxide) and oxidizable (C(sp^3)–OH) functionalities (Fig. 2d). Our target, 4-hydroxy-1,2,3,4-tetrahydroacridine *N*-oxide, was readily synthesized *via* a two-step sequence involving *N*-oxidation and subsequent copper-catalyzed C(sp^3)–H oxidation (Fig. 2e). Upon successful synthesis of this model substrate, its treatment with boric acid or phenylboronic acid remarkably facilitated a one-pot redox transformation (Fig. 2f). This process simultaneously involved the reduction of the azaaryl *N*-oxide to the corresponding azaaromatic and the oxidation of the C(sp^3)–OH group to a ketone, efficiently yielding functionalized 2,3-dihydroacridin-4(1*H*)-ones. Herein, we report a novel, one-pot redox approach for the direct transformation of 4-hydroxy-1,2,3,4-tetrahydroacridine *N*-oxide into a highly functionalized dihydroacridinone using stoichiometric boric acid or phenylboronic acid under mild conditions.

Results and discussion

In pursuit of our objective, 1,2,3,4-tetrahydroacridine *N*-oxide (**2a**) was initially synthesized from tetrahydroacridine (**1a**) *via* an *N*-oxidation using *m*-CPBA in CH_2Cl_2 at 0 °C (see the SI). Subsequently, to generate our target molecule, 4-hydroxy-1,2,3,4-tetrahydroacridine *N*-oxide (**3a**), 1,2,3,4-tetrahydroacridine *N*-oxide was subjected to various copper-catalyzed C(sp^3)–H oxidation reactions, specifically targeting the benzylic position, guided by our prior experience with similar systems.[17,18] Towards this, **2a** was treated with CuI (10 mol%) in the presence of TBHP (*tert*-butyl hydroperoxide; 2 equivalents) as the co-oxidant under an oxygen atmosphere in CH_3CN at 80 °C for 24 h, and the desired product **3a** was obtained with 45% yield (Table 1, entry 1). To optimize the yield of **3a**, we explored various copper and other metal catalysts in different solvents at varying temperatures, as given in Table 1. It is interesting to note that the reaction is working without a co-oxidant but with similar yields (entries 2 and 3). The formation of the desired product was not observed in the absence of a catalyst (entry 4), indicating that the presence of the catalyst is required for the success of the reaction. Solvent screening revealed no reaction in EtOH, H_2O, DCM, and THF (entries 5–8), whereas toluene and xylene proved to be effective, yielding the desired product in 68% and 72%, respectively, in 16 h (entries 9 and 10). Further optimization with DMSO and DMF as solvents at 80 °C and 100 °C led to a significant improvement in the yields to 83%–92% (entries 11–13). Although both DMSO and DMF performed similarly, DMF offered a slight advantage by reducing the reaction time to 2.5 hours, despite slightly lower yields at elevated temperatures (entries 14 and 15). In addition to the solvents, various copper sources [Cu(I) to Cu(II)] like CuCl, CuBr, $CuCl_2{\cdot}H_2O$, $Cu(OAc)_2{\cdot}H_2O$, and $CuSO_4{\cdot}5H_2O$ were evaluated. While all the copper salts produced the desired product, the yields were relatively low (entries 16–20). Alternative metal sources such as $FeCl_2{\cdot}4H_2O$ and $NiCl_2{\cdot}6H_2O$ failed to provide the hydroxyl product

Table 1 Optimization of the reaction conditions[a]

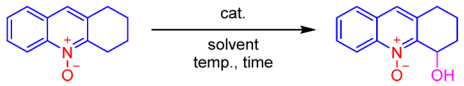

Entry	Catalyst	Solvent	Temp (°C)	Time (h)	Yield[b] (%)
1	CuI[c]	CH_3CN	80	24	45
2	CuI	CH_3CN	80	24	46
3	CuI	CH_3CN	100	24	47
4	—	CH_3CN	80	24	n.r.
5	CuI	EtOH	80	24	n.r.
6	CuI	H_2O	80	24	n.r.
7	CuI	DCM	80	24	n.r.
8	CuI	THF	80	24	Trace
9	CuI	Toluene	80	16	68
10	CuI	Xylene	80	16	72
11	CuI	DMSO	80	6	83
12	CuI	DMSO	100	3	92
13	**CuI**	**DMF**	**100**	**2.5**	**92**
14	CuI	DMF	120	2.5	85
15	CuI	DMF	140	1.5	78
16	CuBr	DMF	80	2	84
17	CuCl	DMF	80	2	85
18	$CuCl_2{\cdot}H_2O$	DMF	80	4	70
19	$Cu(OAc)_2{\cdot}H_2O$	DMF	80	4	70
20	$CuSO_4{\cdot}5H_2O$	DMF	80	4	68
21	$FeCl_2{\cdot}4H_2O$	DMF	80	24	n.r.
22	$NiCl_2{\cdot}6H_2O$	DMF	80	24	n.r.

[a] Reaction conditions: all the reactions were carried out with **2a** (0.3 mmol) and CuI (10 mol%) under an oxygen atmosphere in 2 mL of solvent and conditions mentioned in the table. [b] Isolated yield. [c] TBHP (0.6 mmol) was used. n.r. = no reaction.

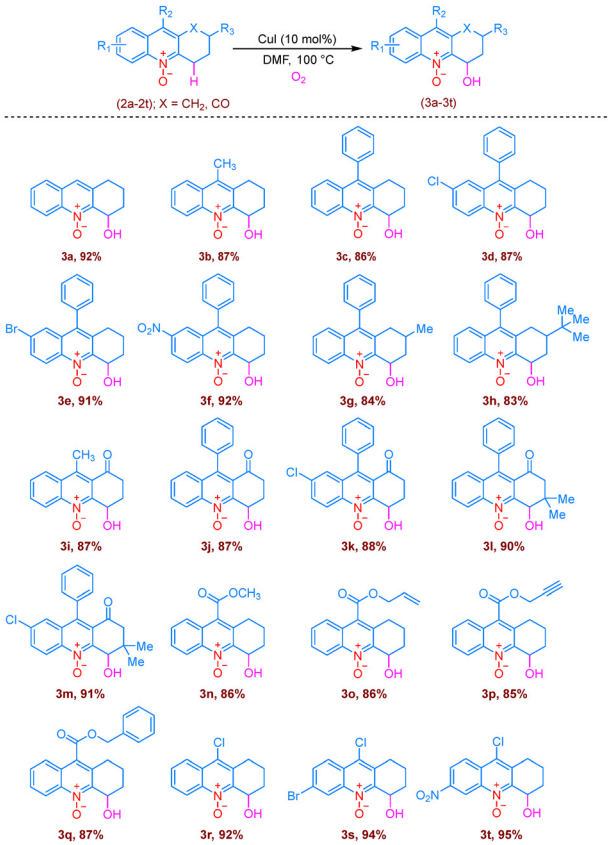

Scheme 1 Substrate scope of 4-hydroxy-1,2,3,4-tetrahydroacridine *N*-oxides. Unless until mentioned, all the reactions were conducted using **2a–2t** (0.3 mmol) and CuI (10 mol%) in 2 mL of DMF under an oxygen atmosphere at 100 °C for 4 to 8 h. The yields are calculated based on the isolated quantities of the product.

(entries 21 and 22). Among the conditions tested, 10 mol% CuI under a molecular oxygen atmosphere in DMF at 100 °C (entry 13) was identified as the optimal condition for this protocol.

Having established the optimal reaction conditions, we prepared a range of substituted tetrahydroacridine *N*-oxides (**2b–2t**) using an established method in our hand and subjected them to benzylic C(sp^3)–H oxidation with CuI (10 mol%) and molecular oxygen (Scheme 1). During this process, it was observed that the substrates bearing substituents such as $-CH_3$ and –Ph at the C9 position reacted efficiently under optimized conditions, yielding the desired products (**3b** and **3c**) in good yields. Notably, electron-withdrawing groups, including –Cl, –Br, and $-NO_2$ at the C7 position, significantly enhance the yields of the oxidized products (**3d–3f**), affording them in excellent yields. Furthermore, substitution at the C2 aliphatic site with methyl and *tert*-butyl groups did not impede the reaction, providing **3g** and **3h** in 84% and 83% yields, respectively. Upon further investigation of the reaction's versatility, we observed that incorporating a keto group at the C1 aliphatic site of the tetrahydroacridine *N*-oxide, alongside substituents such as $-CH_3$ and –Ph at C9 and –Cl at C7, facilitated smooth oxidation, yielding the desired products (**3i–3k**) in excellent yields. Moreover, the presence of a dimethyl group at the C3 position was well-tolerated, affording **3l** and **3m** with high efficiency. It is worth noting that the strong electron-deficient substrates such as methyl, allyl, and propargyl esters at the C9 position were also compatible with this protocol, generating the oxidised products **3n–3p** in good yields. Remarkably, benzyl ester exhibited unique reactivity, undergoing regioselective C4 hydroxylation (**3q**, 87% yield) instead of benzylic oxidation. Finally, substrates with –Cl substitution at C9, or combined substituents at C9 and the aromatic ring (6-Br, 6-NO_2), were smoothly oxidized to the corresponding products (**3r–3t**), achieving excellent yields ranging from 92 to 95%.

Following the successful synthesis of 4-hydroxy-1,2,3,4-tetrahydroacridine *N*-oxides (**3a–3t**), our attention was shifted towards demonstrating the proposed hypothesis (sequential reduction followed by oxidation) by treating 4-hydroxy-1,2,3,4-tetrahydroacridine *N*-oxide (**3a**) with phenylboronic acid (2 equiv.) in DMF at room temperature for 24 h. However, no reduction of the *N*-oxide (**4a′**) nor the oxidation of alcohol product (**4a″**) was observed (Table 2, entry 1). Upon increasing the temperature to 40 °C, the formation of 2,3-dihydroacridin-4(1*H*)-one (**4a**) as the sole redox product was noticed with 35% yield after 24 h, along with unreacted starting material (entry 2). Encouraged by this result, we sought to improve the yield of **4a** by gradually increasing the reaction temperature (from 60 °C to 100 °C). As anticipated, the yield of 2,3-dihydroacridin-4(1*H*)-one (**4a**) was improved to 98% (entries 3–5). Though the yield was greater, the reaction still required a longer time to complete.

Table 2 Optimization of the reaction conditions[a]

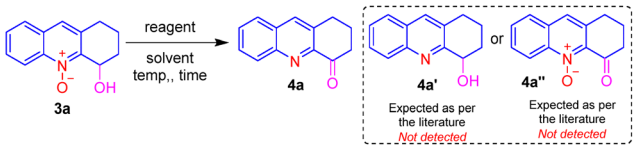

Entry	Reagent	Solvent	Temp. (°C)	Time (h)	Yield[b] (%)
1	$PhB(OH)_2$	DMF	rt	24	n.r.
2	$PhB(OH)_2$	DMF	40	24	35
3	$PhB(OH)_2$	DMF	60	24	44
4	$PhB(OH)_2$	DMF	80	12	98
5	$PhB(OH)_2$	DMF	100	8	98
6	**$PhB(OH)_2$**	**DMF**	**120**	**4**	**98**
7	$PhB(OH)_2$	DMF	140	8	90
8	$PhB(OH)_2$	DMSO	120	4.5	95
9	$PhB(OH)_2$	DMSO	140	12	88
10	$PhB(OH)_2$	Toluene	120	24	78
11	$PhB(OH)_2$	Xylene	120	24	79
12	$PhB(OH)_2$	DCM	120	12	93
13	$PhB(OH)_2$	DCE	120	12	92
14	$PhB(OH)_2$	CH_3CN	120	10	89
15	$PhB(OH)_2$	1,4-Dioxane	120	24	15
16	$PhB(OH)_2$	MeOH	120	24	78
17	$PhB(OH)_2$	H_2O	120	24	n.r.
18	H_3BO_3	DMF	rt	24	Trace
19	H_3BO_3	DMF	80	14	96
20	H_3BO_3	DMF	100	5.5	98
21	**H_3BO_3**	**DMF**	**120**	**4**	**98**

[a] Reaction conditions: all reactions were carried out with **3a** (0.3 mmol) and $PhB(OH)_2$ or H_3BO_3 (0.6 mmol) in 2 mL of solvent and the conditions mentioned in the table. [b] Isolated yields are reported. n.r. = no reaction.

To reduce the reaction time, the experiments were conducted in DMF at elevated temperatures. It was observed that the outcome of the product was the same at 120 °C in 4 h, but increasing the reaction temperature to 140 °C resulted in a decrease in yield. This reduction in yield may be attributed to the decomposition of the reaction complex or intermediate (entry 7). Similar observations were also noticed when dimethyl sulfoxide (DMSO) was employed as a solvent, with no noticeable impact on the generation of the targeted ketone (entries 8 and 9). To investigate further, we conducted experiments in different solvents, but the results were not promising (entries 10–14). Notably, 1,4-dioxane proved unsuitable due to poor solubility of the starting material, leading to a low product yield (entry 15). Subsequently, a transition from aprotic solvents to protic solvents, specifically methanol (MeOH) and water (H_2O), was explored (entries 16 and 17). This alteration resulted in a satisfactory product yield in the case of MeOH, while the use of aqueous media showed no significant improvement in the progress of the reaction. To simplify the reaction conditions, we also investigated boric acid as a reagent, conducting a temperature study from 80 to 120 °C in DMF (entries 18–21). Ultimately, we found that 2 equivalents of either phenylboronic acid or boric acid in DMF at 120 °C represented the optimal conditions, providing excellent yields of the corresponding ketone (**4a**) (Scheme 2).

After establishing the optimal conditions, we explored the broader applicability of the developed strategy by testing a

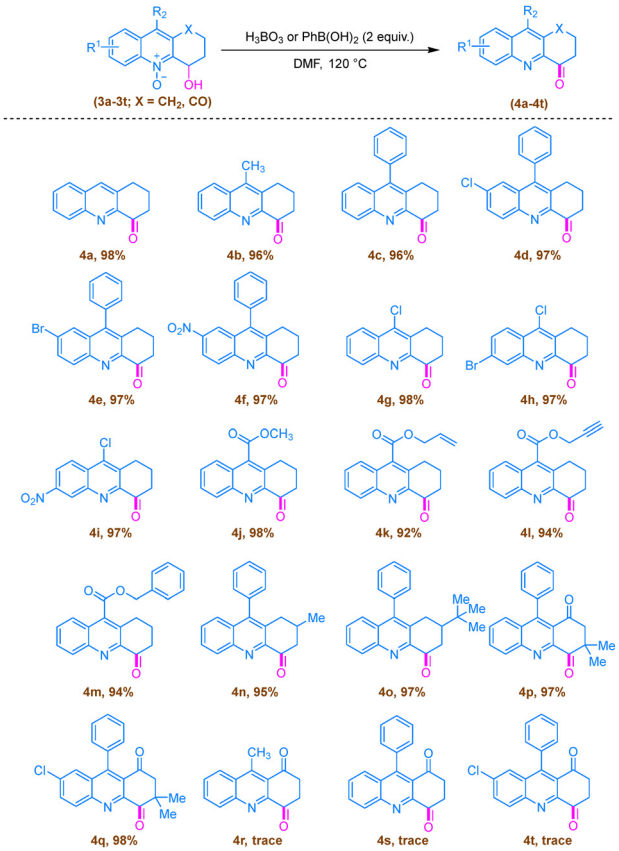

Scheme 2 Substrate scope of 2,3-dihydroacridin-4(1*H*)-ones. Unless until mentioned, all the reactions were conducted using **3a–3t** (0.3 mmol) and $PhB(OH)_2$ or H_3BO_3 (0.6 mmol) in 2 mL of DMF at 120 °C for 8 to 12 h. The yields are calculated based on the isolated quantities of the product.

range of substituted 4-hydroxy-1,2,3,4-tetrahydroacridine *N*-oxides (Scheme 3). This protocol exhibited robust performance for various types of substituents, including both electron-withdrawing and electron-donating substituents at C7 and C9 positions. For example, substituents such as $-CH_3$ (**4b**), –Ph (**4c**) and –COOR groups at the C9 position (**4j–4m**) led to excellent yields. The presence of electron-withdrawing groups like Cl, Br, and NO_2 at the aromatic C7 position (**4d–4f**) did not adversely affect the productivity of the desired yield. Moreover, the

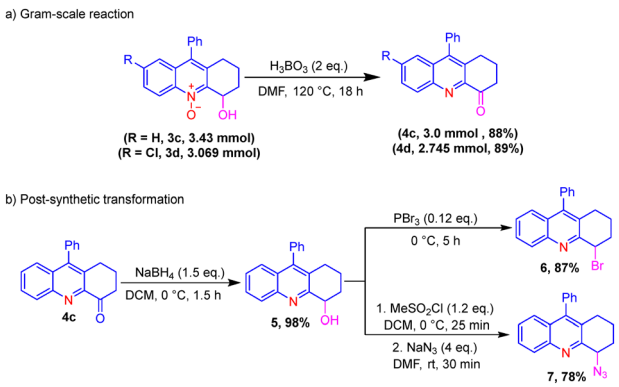

Scheme 3 (a) Gram-scale reaction; (b) post-synthetic modification.

introduction of halogen groups like Cl at C9, alongside another halogen (Br), and strong electron-withdrawing groups like NO_2 at C6 (**4g–4i**), did not negatively impact the reaction outcome. We also observed comparable reactivity with sterically hindered substituents like $-CH_3$ and $-C(CH_3)_3$ at the C2 position (**4n–4o**). Additionally, when the keto group was present at the C1 position and a dimethyl group at C3, diketones (**4p–4t**) were produced in excellent yields. However, when attempting to synthesize diketones with no functional groups at the C3 position, only trace amounts were obtained, as confirmed by HMRS data.

Later, a gram scale experiment was carried out using **3c** or **3d** and boric acid in DMF (10 mL) at 120 °C. The corresponding ketone **4c** or **4d** was successfully obtained with a yield of 88% and 89% as depicted in Scheme 3. Furthermore, given applications of 2,3-dihydroacridin-4(1*H*)-ones as ligands in metal catalysis[19] and as intermediates in lactam synthesis,[20] the synthetic utility of compound **4c** was further explored by reducing it to the corresponding hydroxyl product (**5**), which was obtained in 98% yield. Similarly, the treatment of **5** with PBr_3 led to the formation of the product (**6**) with 87% yield. In addition, product (**5**) was transformed to azide (**7**) in 78% yield as shown in Scheme 3. Both the products (**6**) and (**7**) can be used for further functionalization, like cross-coupling and click chemistry (that is in progress in our laboratory as a part of our ongoing medicinal chemistry program) to generate a library of compounds for the acetyl/butyryl cholinesterase inhibition. To understand the reaction mechanism of the boric acid or boronic acid-mediated novel redox reaction, the isolation of the intermediates and further experiments were performed. Towards this, initially, the reaction of 4-hydroxy-9-phenyl-1,2,3,4-tetrahydroacridine *N*-oxide (**3c**) and boric/boronic acid was performed under optimal conditions (Scheme 4). After careful investigation, we found the *N*-oxide reduced intermediate 9-phenyl-1,2,3,4-tetrahydroacridin-4-ol (Scheme 4a) (see the SI). Then, the same reaction was performed under an inert atmosphere by using a nitrogen or argon environment to afford the desired redox product (**4c**), which eliminates the role of oxygen in the oxidation process. In this context, a separate experiment was also conducted with the *N*-oxide reduced product using boric/phenylboronic acid (Scheme 4c and d). But surprisingly, when the same condition was applied for different alcohols (with benzylic carbon), no oxidative product was observed, which indicates that the absence of the ring nitrogen was playing a key role and hampered the oxidative process (Scheme 4e–i). In addition, an experiment was conducted with 1,2,3,4-tetrahydroanthracen-1-ol; no oxidation was observed, supporting the aforementioned conclusion (Scheme 4j).

To support the hypothesis and experimental results, a DFT study was carried out to understand the role of the ring nitrogen in the oxidation. Furthermore, we monitored the reaction by conducting NMR experiments, where 4-hydroxy-9-phenyl-1,2,3,4-tetrahydroacridine *N*-oxide was exposed to 2 equiv. of boric acid in DMSO-d_6 at room temperature, which is shown in Fig. 3. No additional precaution has been taken, such as an inert atmosphere or anhydrous conditions. The ^{1}H

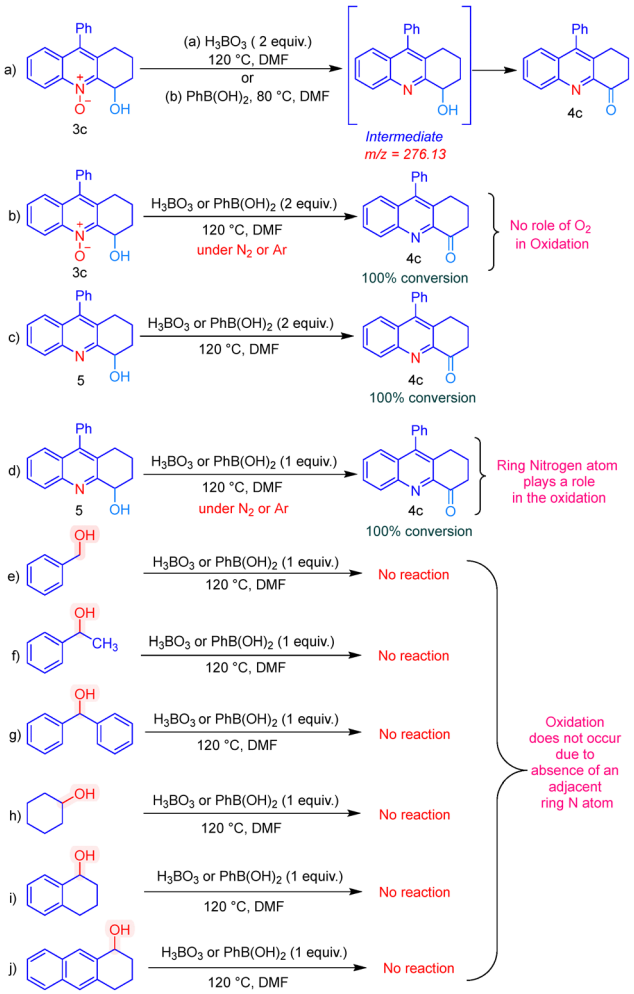

Scheme 4 Mechanistic studies.

and ^{11}B NMR experiments were performed using 4-hydroxy-9-phenyl-1,2,3,4-tetrahydroacridine *N*-oxide (**3c**; 0.1 mmol) in DMSO-d_6 (0.5 mL) treated with H_3BO_3 (2 equiv.). In Fig. 3, a gradual disappearance of the NMR signal at δ = 8.51–8.53 ppm corresponding to CH($\mathbf{H_A}$) of C5 carbon of 4-hydroxy-1,2,3,4 *N*-oxide was observed with the simultaneous appearance of the NMR signal at δ = 8.20–8.22 ppm corresponding to CH($\mathbf{H_D}$) of 9-phenyl-2,3-dihydroacridin-4(1*H*)-one due to the reduction of *N*-oxide. This is accompanied by the disappearance of the NMR signal at δ = 5.35 ppm due to aliphatic CH($\mathbf{H_B}$) of C4 attached to –OH($\mathbf{H_C}$) as well as a signal at δ = 6.55 ppm due to the oxidation of the hydroxyl group at C4 into a ketone in 0 to 120 minutes.

More profoundly, 2D spectra (NOESY and HMQC) of the starting materials, intermediates, and final products were recorded and compared, where a gradual upfield shift of C5, loss of the carbinol resonance, and downfield shift of the methylene C3 alpha to the carbonyl can be observed (see the SI). In addition, the ^{11}B NMR signal was seen at δ = 19.91 ppm, but not conclusive (for more details, see the SI). These experiments clearly indicate that the reduction of *N*-oxide is preferred over the oxidation of secondary alcohol in the reaction sequence.

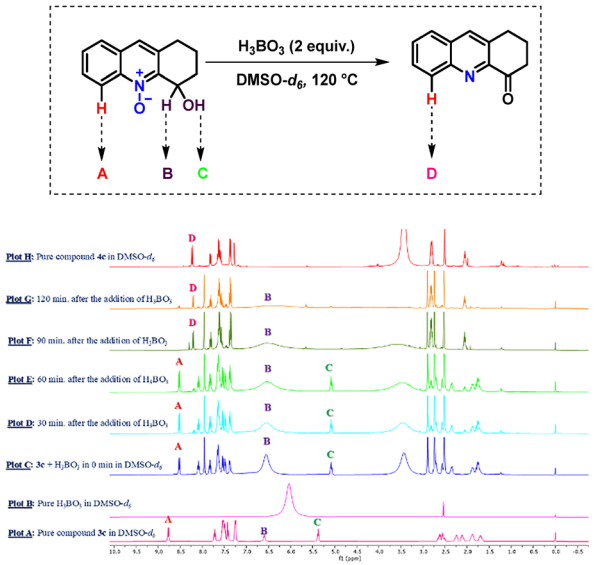

Fig. 3 ^{1}H NMR experiments to probe the reaction intermediates.

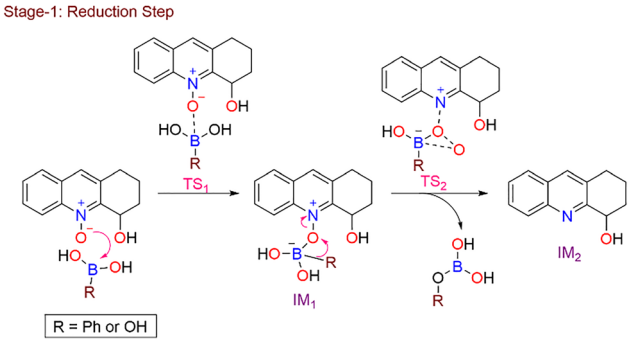

Fig. 4 Proposed mechanism for the reduction reaction.

In light of experimental evidence, the mechanism of the redox reaction between 4-hydroxy-1,2,3,4-tetrahydroacridine *N*-oxide and H_3BO_3 has been considered in two stages, *i.e.*, reduction and oxidation stages respectively, and computationally investigated. In the reduction step, referred to as Stage 1 (see Fig. 4), the empty p-orbital on the boron atom of boronic acid makes it susceptible to nucleophilic attack by reactive oxygen species, such as *N*-oxide. This attack results in a 1,2 shift of either the phenyl or the hydroxyl group from the boron atom, leading to the formation of a boronic ester. This boronic ester then rapidly undergoes hydrolysis to regenerate boronic acid. This mechanism is supported by the work of H. G. Kuivila,[21] which investigated the kinetics of the reaction between phenylboronic acid and hydrogen peroxide. The kinetic studies suggested the likelihood of a 1,2 shift of the phenyl group to form the phenylboronic ester. Notably, the 1,2 shift was identified as the rate-limiting step of the reaction. Additionally, the formation of phenol during the reduction of *N*-oxides has been previously reported,[13] further supporting our proposed mechanism. All the possible structures shown in Fig. 4, *i.e.*, TS1, IM1, TS2, and IM2, were modelled and fully optimized using the ωB97XD functional employing the 6-31+g(d) basis set.[22] The vibrational frequency calculations have been carried out to unveil the nature of the stationary points as local minima and as saddle points.

The transition states were confirmed by the presence of a single imaginary frequency. The optimized geometries were then used to study the energy changes occurring in the reaction. All the calculations have been carried out using the Gaussian 16 software package.[23] The relative free energy profile along with the labelled optimized structures for the Stage 1 reaction is shown in Fig. 5. It can be seen from Fig. 5 that 6.7 kcal mol^{-1} energy is needed for the interaction of O and B to give IM1 *via* TS1. The relative energy of IM1 is 6.4 kcal mol^{-1}, which is slightly lower than the relative energy of TS1. Also, the

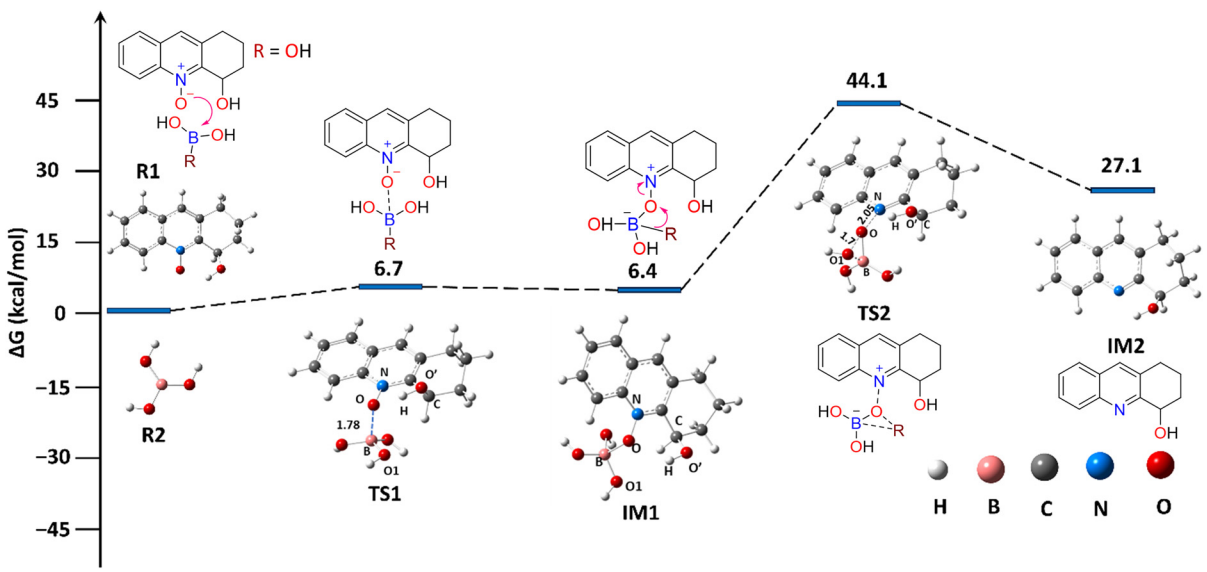

Fig. 5 Relative free energy profile for Stage 1 with all the optimized structures.

positive free energy change of the reaction shows that IM1 is readily active and undergoes a 1,2-shift of the –OH group to yield IM2 through TS2. The energy barrier for this step was found to be 44.1 kcal mol^{-1}. This shows that the shifting of the –OH group at H_3BO_3 is the rate-determining step in the reduction of R1, which is in agreement with the previous reports.[21] In addition to this, the relative energy of IM2 was 27.1 kcal mol^{-1}, signifying the endergonic nature of Stage 1. To the best of our knowledge, there have been no detailed mechanistic investigations into the oxidation of hydroxyl groups using boronic acids. The work by William *et al.*[16b] provides the first evidence of hydroxyl group oxidation catalyzed by boronic acid. They observed that the activation of 1,2-diols by boronic acid, through the formation of boronate esters, leads to the production of α-hydroxy ketones, facilitated by the presence of an electro-generated OH^- ion at the cathode. This research offers insights into the initiation of the oxidation reaction, specifically the formation of a boronate ester-like moiety through the condensation of the hydroxyl group with boronic acid. We further verified the possibility of this condensation by comparing it to the nucleophilic attack on the boron atom by the lone pair of the N atom (see Fig. 6). The relative energy profile in Fig. 6 indicates that the nucleophilic attack requires 7.9 kcal mol^{-1} more energy than the condensation reaction, resulting in a less stable intermediate (IM3′) compared to IM3. This suggests that condensation may indeed be the initial step in the oxidation reaction. The condensation product, IM3, can further transform into IM4 through the interaction of lone pairs on the nitrogen atom and the empty p_z orbitals on the boron atom, *via* the transition state TS4. The intermediate IM4 was found to be 2.3 kcal mol^{-1} more stable than IM3, requiring only 1 kcal mol^{-1} for its formation (see Fig. 7). The donation of a lone pair from the nitrogen atom to the boron atom leads to electron deficiency at the nitrogen, which can be compensated by the transfer of π

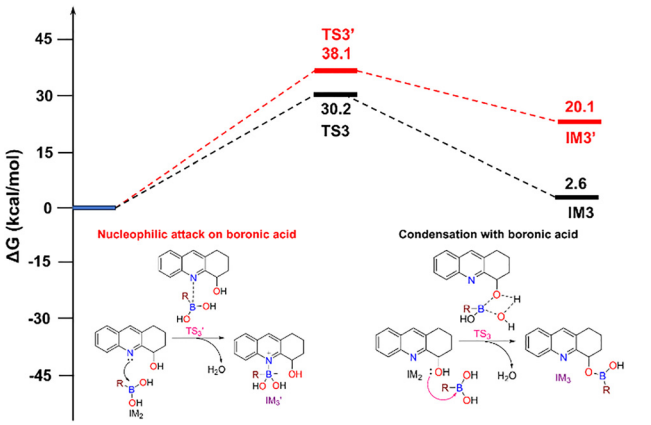

Fig. 6 Comparison of nucleophilic attack and the condensation possibilities in the reaction of IM3 with boronic acid for the oxidation stage.

electrons from the nitrogen–carbon double bond. This transfer creates an electron deficiency at the adjacent carbon atom, as confirmed by natural population analysis (NPA), which shows a charge of $0.231e^-$ on the carbon atom. This electron deficiency increases the acidity of the hydrogen atom at the C4 position, making it more susceptible to abstraction. The proton abstraction may then be facilitated by the OH^- ion generated from the reaction between water (released in the condensation step) and boronic acid. The abstraction of H^+ leads to the formation of IM5, which resembles oxazaborolidines. The deprotonation of IM4 by OH^- is an underbarrier reaction. The relative energy of TS5 was found to be −17.8 kcal mol^{-1}, which further gives IM5 with a relative energy of −51.1 kcal mol^{-1}. Natural bond orbital (NBO) analysis reveals that in IM5, the nitrogen atom is not fully sp^3 hybridized, exhibiting sp^2 hybridization instead. Additionally, the expected lone pair on the nitrogen atom appears to be in conjugation rather than fully present, indicating

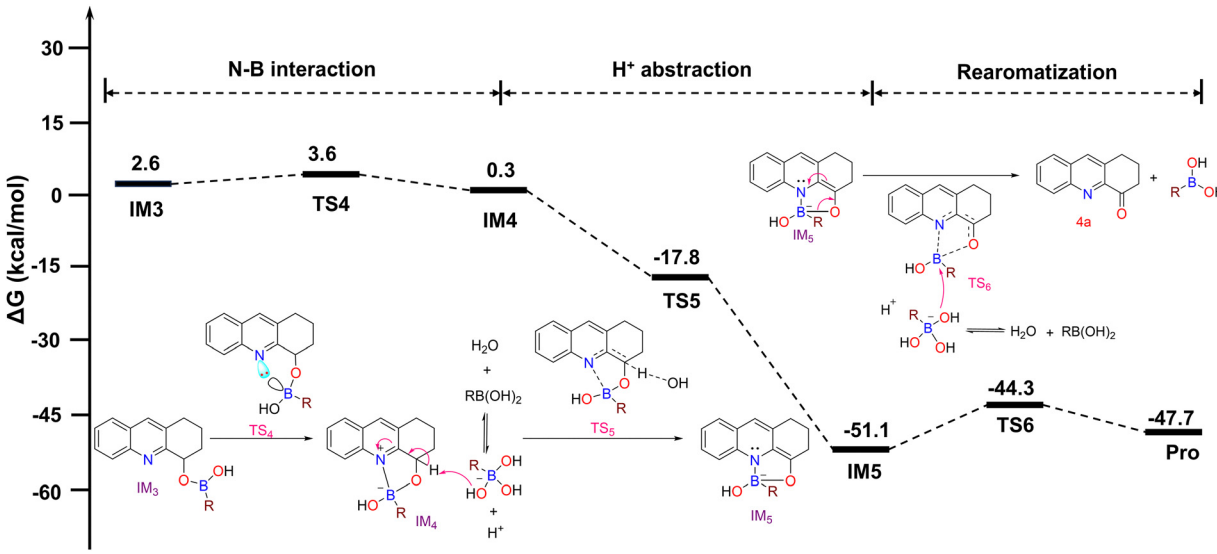

Fig. 7 Relative energy profile and the proposed mechanism for the oxidation reaction.

a change in the aromatic character of the molecule. To restore aromaticity, an electronic rearrangement *via* the oxazaborolidine ring opening is expected in subsequent steps.

It has been established that in oxazaborolidines, the N–B bond can open for enantiotopomerization,[24] suggesting the possibility of N–B bond opening in IM5. For aromaticity restoration, the B–O bond may also open. We systematically compared the possibilities of N–B and B–O bond openings (shown in Fig. S1 in the SI) and found that the opening of the N–B bond requires approximately 5 kcal mol^{-1} more energy than the B–O bond opening. Therefore, B–O bond opening may be preferred, leading to the expected formation of IM5′ and boronic acid through the attack of OH^-. Although we attempted to optimize the expected intermediate IM5′ resulting from the B–O bond opening, the optimization reverted to IM5. This indicates the instability of the expected intermediate (*i.e.*, IM5′) and suggests that further steps may occur simultaneously. Thus, electronic rearrangement *via* B–O bond opening for rearomatization is likely to take place in the presence of the borate anion formed from the reaction of water and boronic acid. The intermediate IM5 yields the oxidized product with the requirement of ∼7 kcal mol^{-1} energy *via* TS6. The optimized geometries of the structures observed in the oxidation stage are given in Fig. S2 of the SI along with the Cartesian coordinates. Based on our experimental results and the absence of previous reports on the oxidation mechanism, we have proposed a plausible mechanism that could pave the way for future research in the investigation of the oxidation mechanism.

Conclusions

In conclusion, this study illustrates a novel redox application of boric and/or boronic acids in the 1,2,3,4-tetrahydroacridine framework. This methodology enables efficient reduction of *N*-oxide functionalities into azaaromatic compounds and concurrent oxidation of benzylic hydroxyl groups to ketones in 4-hydroxy-1,2,3,4-tetrahydroacridine *N*-oxides, delivering 2,3-dihydroacridin-4(1*H*)-ones with outstanding efficiency, excellent yields, and high tolerance to various functional groups. The method displays broad substrate scope, excellent chemoselectivity, and scalability, providing access to structurally diverse tetrahydroacridine scaffolds relevant to medicinal and materials chemistry. Detailed mechanistic investigations, supported by density functional theory (DFT) calculations, elucidate the underlying redox pathways and offer valuable insights into the unique boron-mediated transformations.

Conflicts of interest

There are no conflicts to declare.

Data availability

The characterization/analytical data of all the compounds are available with the article as supplementary information (SI). Supplementary information is available. See DOI: https://doi.org/10.1039/d5nj03387j.

Acknowledgements

TS and SM thank MoE, India for the fellowship. DK acknowledges DST (SERB), New Delhi, India for the financial support (SB/FT/CS-136/2012 and SB/EMEQ-103/2014).

References

1 (*a*) N. Kerru, L. Gummidi, S. Madddila, K. K. Gangu and S. B. Jonnalagadda, A Review on Recent Advances in Nitrogen-Containing Molecules and Their Biological Applications, *Molecules*, 2020, **25**, 1909; (*b*) M. M. Heravi and V. Zadsirjan, Prescribed drugs containing nitrogen heterocycles: an overview, *RSC Adv.*, 2020, **10**, 44247–44311; (*c*) O. O. Ajani, K. T. Lyaye and O. T. Ademosun, Recent advances in chemistry and therapeutic potential of functionalized quinoline motifs–a review, *RSC Adv.*, 2022, **12**, 18594–18614; (*d*) A. Kumar, A. K. Singh, H. Singh, V. Vijayan, D. Kumar, J. Naik, S. Thareja, J. P. Yadav, P. Pathak, M. Grishina, A. Verma, H. Khalilullah, M. Jaremko, A. H. Emwas and P. Kumar, Nitrogen Containing Heterocycles as Anticancer Agents: A Medicinal Chemistry Perspective, *Pharmaceuticals*, 2023, **16**, 299; (*e*) S. Majee, Shilpa, M. Sarav, B. K. Banik and D. Ray, Recent Advances in the Green Synthesis of Active N-Heterocycles and Their Biological Activities, *Pharmaceuticals*, 2023, **16**, 873; (*f*) K. T. Jha, A. Shome, Chahat and P. A. Chawla, Recent advances in nitrogen-containing heterocyclic compounds as receptor tyrosine kinase inhibitors for the treatment of cancer: Biological activity and structural activity relationship, *Bioorg. Chem.*, 2023, **138**, 106680; (*g*) W. Luo, Y. Liu, H. Qin, Z. Zhao, S. Wang, W. He, S. Tang and J. Peng, Nitrogen-containing heterocyclic drug products approved by the FDA in 2023: Synthesis and biological activity, *Eur. J. Med. Chem.*, 2024, **279**, 116838; (*h*) A. Leśniewska and P. Przybylski, Seven-membered N-heterocycles as approved drugs and promising leads in medicinal chemistry as well as the metal-free domino access to their scaffolds, *Eur. J. Med. Chem.*, 2024, **275**, 116556; (*i*) C. M. Marshall, J. G. Federice, C. N. Bell, P. B. Cox and J. T. Njardarson, An Update on the Nitrogen Heterocycle Compositions and Properties of U.S. FDA-Approved Pharmaceuticals (2013–2023), *J. Med. Chem.*, 2024, **67**, 11622–11655; (*j*) Mallapa, M. Chahar, N. Choudhary, K. K. Yadav, M. T. Qasim, R. Zairov, A. Patel, V. K. Yadav and M. Jangir, Recent advances in the synthesis of nitrogen-containing heterocyclic compounds via multicomponent reaction and their emerging biological applications: a review, *J. Iran. Chem. Soc.*, 2025, **22**, 1–33.

2 (*a*) M. Gensicka-Kowalewska, G. Cholewiński and K. Dzierzbicka, Recent developments in the synthesis and biological activity of acridine/acridone analogues, *RSC Adv.*,

2017, **7**, 15776–15804; (*b*) P. R. Carlier, E. S. H. Chow, Y. Han, J. Liu, J. E. Yazal and Y. P. Pang, Heterodimeric Tacrine-Based Acetylcholinesterase Inhibitors: Investigating Ligand−Peripheral Site Interactions, *J. Med. Chem.*, 1999, **42**, 4225–4231; (*c*) P. Camps, R. E. Achab, J. Morral, D. Munoz-Torrero, A. Badia, J. Eladi Banos, N. M. Vivas, X. Barril, M. Orozco and F. Javier Luque, New Tacrine−Huperzine A Hybrids (Huprines): Highly Potent Tight-Binding Acetylcholinesterase Inhibitors of Interest for the Treatment of Alzheimer's Disease, *J. Med. Chem.*, 2000, **43**, 4657–4666; (*d*) B. Sameem, M. Saeedi, M. Mahdavi and A. Shafiee, A review on tacrine-based scaffolds as multi-target drugs (MTDLs) for Alzheimer's disease, *Eur. J. Med. Chem.*, 2017, **128**, 332–345; (*e*) K. Czarnecka, N. Chufarova, K. Halczuk, K. Maciejewska, M. Girek, R. Skibiński, J. Jończyk, M. Bajda, J. Kabziński, I. Majsterek and P. Szymański, Tetrahydroacridine derivatives with dichloronicotinic acid moiety as attractive, multipotent agents for Alzheimer's disease treatment, *Eur. J. Med. Chem.*, 2018, **145**, 760–769; (*f*) K. Czarnecka, M. Girek, P. Wójtowicz, P. Kręcisz, R. Skibiński, J. Jończyk, K. Łątka, M. Bajda, A. Walczak, G. Galita, J. Kabziński, I. Majsterek, P. Szymczyk and P. Szymański, New Tetrahydroacridine Hybrids with Dichlorobenzoic Acid Moiety Demonstrating Multifunctional Potential for the Treatment of Alzheimer's Disease, *Int. J. Mol. Sci.*, 2020, **21**, 3765; (*g*) P. Varakumar, K. Rajagopal, B. Aparna, K. Raman, G. Byran, C. M. Gonçalves Lima, S. Rashid, M. H. Nafady, T. B. Emran and S. Wybraniec, Acridine as an Anti-Tumour Agent: A Critical Review, *Molecules*, 2023, **28**, 193; (*h*) J. Zhu, H. Yang, Y. Chen, H. Lin, Q. Li, J. Mo, Y. Bian, Y. Pei and H. Sun, Synthesis, pharmacology and molecular docking on multifunctional tacrine-ferulic acid hybrids as cholinesterase inhibitors against Alzheimer's disease, *J. Enzyme Inhib. Med. Chem.*, 2018, **33**, 496–506.

3 (*a*) T. Shirisha, S. Majhi, K. Divakar and D. Kashinath, Metal-free synthesis of functionalized tacrine derivatives and their evaluation for acetyl/butyrylcholinesterase and α-glucosidase inhibition, *Org. Biomol. Chem.*, 2024, **22**, 790–804; (*b*) T. Shirisha, S. Majhi, K. Divakar and D. Kashinath, Synthesis of C4-functionalized 1,2,3,4-tetrahydroacridine-based Pfitzinger acid derivatives in deep eutectic solvents and their biological evaluation as dual cholinesterase and α-glucosidase inhibitors, *New J. Chem.*, 2025, **49**, 1072–1082; (*c*) T. Shirisha, S. Majhi, K. Divakar and D. Kashinath, Synthesis of 1,2,3,4-tetrahydroacridine based 1,2,3-triazole derivatives and their biological evaluation as dual cholinesterase and α-glucosidase inhibitors, *New J. Chem.*, 2025, **49**, 14381–14387.

4 (*a*) J. Waluk, J. Herbich, R. P. Thummel, A. Gorski, K. Nawara and B. Golec, Combined effect of hydrogen bonding interactions and freezing of rotameric equilibrium on the enhancement of photostability, *Phys. Chem. Chem. Phys.*, 2018, **20**, 13306–13315; (*b*) N. Tka, M. A. H. Ayed, M. B. Braiek, M. Jabli, N. Chaaben, K. Alimi, S. Jopp and P. Langer, 2,4-Bis(arylethynyl)-9-chloro-5,6,7,8-tetrahydroacridines: synthesis and photophysical properties, *Beilstein J. Org. Chem.*, 2021, **17**, 1629–1640; (*c*) N. Tka, M. A. H. Ayed, M. B. Braiek, M. Jabli and P. Langer, Synthesis and investigation on optical and electrochemical properties of 2,4-diaryl-9-chloro-5,6,7,8-tetrahydroacridines, *Beilstein J. Org. Chem.*, 2021, **17**, 2450–2461.

5 (*a*) M. Kobus, T. Friedrich, E. Zorn, N. Burmeister and W. Maison, Medicinal Chemistry of Drugs with N-oxide Functionalities, *J. Med. Chem.*, 2024, **67**, 5168–5184; (*b*) Y. Dubey and S. Kanvah, Fluorescent N-oxides: applications in bioimaging and sensing, *Org. Biomol. Chem.*, 2024, **22**, 7582–7595.

6 (*a*) N. Miyaura and A. Suzuki, Palladium-Catalyzed Cross-Coupling Reactions of Organoboron Compounds, *Chem. Rev.*, 1995, **95**, 2457–2483; (*b*) A. Suzuki, Cross-Coupling Reactions Of Organoboranes: An EasyWay To Construct C–C Bonds (Nobel Lecture), *Angew. Chem., Int. Ed.*, 2011, **50**, 6722–6737; D. G. Brown and J. Boström, Analysis of Past and Present Synthetic Methodologies on Medicinal Chemistry: Where Have All the New Reactions Gone?, *J. Med. Chem.*, 2016, **59**, 4443–4458; (*c*) I. P. Beletskaya, F. Alonso and V. Tyurin, The Suzuki-Miyaura reaction after the Nobel prize, *Coord. Chem. Rev.*, 2019, **385**, 137–173.

7 B. J. Graham and R. T. Raines, Emergent Organoboron Acid Catalysts, *J. Org. Chem.*, 2024, **89**, 2069–2089.

8 (*a*) D. G. Hall, *Boronic Acids: Preparation and Applications in Organic Synthesis, Medicine and Materials*, 2nd edn, Wiley−VCH, Weinheim, Germany, 2011; (*b*) H. Zheng and D. G. Hall, Boronic Acid Catalysis: An Atom-Economical Platform for Direct Activation and Functionalization of Carboxylic Acids and Alcohols, *Aldrichimica Acta*, 2014, **47**, 41–51; (*c*) D. G. Hall, Boronic acid catalysis, *Chem. Soc. Rev.*, 2019, **48**, 3475–3496.

9 (*a*) E. Dimitrijevic and M. S. Taylor, Organoboron Acids and Their Derivatives as Catalysts for Organic Synthesis, *ACS Catal.*, 2013, **3**, 945–962; (*b*) M. S. Taylor, Catalysis Based on Reversible Covalent Interactions of Organoboron Compounds, *Acc. Chem. Res.*, 2015, **48**, 295–305.

10 (*a*) V. Nori, F. Pesciaioli, A. Sinibaldi, G. Giorgianni and A. Carlone, Boron-Based Lewis Acid Catalysis: Challenges and Perspectives, *Catalysts*, 2022, **12**, 5; (*b*) S. Tu, F. Fang, C. Miao, H. Jiang, Y. Feng, D. Shi and X. Wang, One-pot synthesis of 3,4-dihydropyrimidin-2(1*H*)-ones using boric acid as catalyst, *Tetrahedron Lett.*, 2003, **44**, 6153–6155.

11 (*a*) K. Ishihara, H. Kurihara and H. Yamamoto, Diarylborinic Acids as Efficient Catalysts for Selective Dehydration of Aldols, *Synlett*, 1997, 597–599; (*b*) R. M. Al-Zoubi, O. Marion and D. G. Hall, Direct and Waste-Free Amidations and Cycloadditions by Organocatalytic Activation of Carboxylic Acids at Room Temperature, *Angew. Chem., Int. Ed.*, 2008, **47**, 2876–2879; (*c*) H. Zheng and D. G. Hall, Mild and efficient boronic acid catalysis of Diels–Alder cycloadditions to 2-alkynoic acids, *Tetrahedron Lett.*, 2010, **51**, 3561–3564; (*d*) K. A. D'Angelo and M. S. Taylor, Borinic Acid Catalyzed Stereo- and Regioselective Couplings of Glycosyl Methanesulfonates, *J. Am. Chem. Soc.*, 2016, **138**, 11058–11066.

12 (*a*) H. P. Kokatla, P. F. Thomson, S. Bae, V. R. Doddi and M. K. Lakshman, Reduction of Amine N-oxides by Diboron Reagents, *J. Org. Chem.*, 2011, **76**, 7842–7848; (*b*) A. Londregan, D. Piotrowski and J. Xiao, Rapid and Selective in situ Reduction of Pyridine-N-oxides with Tetrahydroxydiboron, *Synlett*, 2013, 2695–2700; (*c*) J. Kim and C. R. Bertozzi, A Bioorthogonal Reaction of N-oxide and Boron Reagents, *Angew. Chem., Int. Ed.*, 2015, **54**, 15777–15781; (*d*) M. R. Andrzejewska, P. K. Vuram, N. Pottabathini, V. Gurram, S. S. Relangi, K. A. Korvinson, R. Doddipalla, L. Stahl, M. C. Neary, P. Pradhan, S. Sharma and M. K. Lakshman, The Disappearing Director: The Case of Directed N-Arylation via a Removable Hydroxyl Group, *Adv. Synth. Catal.*, 2018, **360**, 2503–2510.

13 S. Gupta, S. Popuri, A. D. Singh, S. Sabiah and J. Kandasamy, Deoxygenation of tertiary amine N-oxides under metal free condition using phenylboronic acid, *Tetrahedron Lett.*, 2017, **58**, 909–913.

14 A. Chardon, O. Maubert, J. Rouden and J. Blanchet, Metal-Free Reduction of Phosphine Oxides, Sulfoxides, and N-oxides with Hydrosilanes using a Borinic Acid Precatalyst, *ChemCatChem*, 2017, **9**, 4460–4464.

15 (*a*) R. K. Mylavarapu, K. Gcm, N. Kolla, R. Veeramalla, P. Koilkonda, A. Bhattacharya and R. Bandichhor, Metal-Free Reduction of Phosphine Oxides, Sulfoxides, and N-oxides with Hydrosilanes using a Borinic Acid Precatalyst, *Org. Process Res. Dev.*, 2007, **11**, 1065–1068; (*b*) M. T. Sabatini, T. Lee, D. B. Tom and L. Sheppard, Borate esters: Simple catalysts for the sustainable synthesis of complex amides, *Sci. Adv.*, 2017, **3**, e1701028.

16 (*a*) A. Rostami and J. Akradi, A highly efficient, green, rapid, and chemoselective oxidation of sulfides using hydrogen peroxide and boric acid as the catalyst under solvent-free conditions, *Tetrahedron Lett.*, 2010, **51**, 3501–3503; (*b*) J. M. William, M. Kuriyama and O. Onomura, Boronic Acid-Catalyzed Selective Oxidation of 1,2-Diols to α-Hydroxy Ketones in Water, *Adv. Synth. Catal.*, 2014, **356**, 934–940.

17 (*a*) H. Y. Kim and K. Oh, Recent advances in the copper-catalyzed aerobic $C_{sp}{}^3$–H oxidation strategy, *Org. Biomol. Chem.*, 2021, **19**, 3569–3583; (*b*) S. E. Allen, R. R. Walvoord, R. Padilla-Salinas and M. C. Kozlowski, Aerobic Copper-Catalyzed Organic Reactions, *Chem. Rev.*, 2013, **113**, 6234–6458; (*c*) T. Punniyamurthy and L. Rout, Recent advances in copper-catalyzed oxidation of organic compounds, *Coord. Chem. Rev.*, 2008, **252**, 134–154.

18 (*a*) T. Shirisha, S. Majhi and D. Kashinath, TBAI-TBHP Mediated C4-Selective C(sp^3)-H Sulfonylation of 1,2,3,4-Tetrahydroacridines and Oxidative Desulfonylation to 2,3-Dihydro Acridin-4(1*H*)-Ones, *ChemistrySelect*, 2024, **9**, e202403503; (*b*) T. Shirisha, S. Majhi, S. Balasubramanian and D. Kashinath, Metal-free C(sp^3)–H functionalization (C–C and C–N bond formation) of 1,2,3,4-tetrahydroacridines using deep eutectic solvents as catalyst and reaction medium, *Org. Biomol. Chem.*, 2024, **22**, 1434–1440; (*c*) T. Shirisha, S. Majhi and D. Kashinath, One-Pot Synthesis of Functionalized Carbazoles and β-Carbolines via Diethyl Azodicarboxylate Mediated Dehydrogenative Aromatization in Deep Eutectic Solvent, *ChemistrySelect*, 2024, **9**, e202401275.

19 (*a*) F. Soccolini, G. Sanna, A. Saba and G. Chelucci, Tetrahedron Chiral 2,2′-bipyridines, 5,6-dihydro-1,10-phenanthrolines and 1,10-phenanthrolines as ligands for enantioselective palladium catalyzed allylic substitution, *Asymmetry*, 2000, **11**, 3427–3438; (*b*) F. Wu and R. P. Thummel, Ru(II) complexes of crowded delocalized diimine ligands, *Inorg. Chim. Acta.*, 2002, **327**, 26–30; (*c*) Y.-Z. Hu, G. Zhang and R. P. Thummel, Friedländer Approach for the Incorporation of 6-Bromoquinoline into Novel Chelating Ligands, *Org. Lett.*, 2003, **5**, 2251–2253; (*d*) J. Dou, D. Zhu, W. Zhang, R. Wang, S. Wang, Q. Zhang, X. Zhang and W.-H. Sun, Highly efficient iron(II) catalysts toward ring opening polymerization of ε-caprolactone through in situ initiation, *Inorg. Chim. Acta.*, 2019, **488**, 299–303.

20 N. Wang, Q.-S. Gu, Z.-L. Li, Z. Li, Y.-L. Guo, Z. Guo and X. Y. Liu, Direct Photocatalytic Synthesis of Medium-Sized Lactams by C−C Bond Cleavage, *Angew. Chem., Int. Ed.*, 2018, **57**, 14225–14229.

21 H. Kuivila, Electrophilic Displacement Reactions. III. Kinetics of the Reaction between Hydrogen Peroxide and Benzeneboronic Acid, *J. Am. Chem. Soc.*, 1954, **76**, 870–874.

22 J.-D. Chai and M. Head-Gordon, Long-Range Corrected Hybrid Density Functionals with Damped Atom–Atom Dispersion Corrections, *Phys. Chem. Chem. Phys.*, 2008, **10**, 6615.

23 M. J. Frisch, G. W. Trucks, H. B. Schlegel, G. E. Scuseria, M. A. Robb, J. R. Cheeseman, G. Scalmani, V. Barone, G. A. Petersson, H. Nakatsuji, X. Li, M. Caricato, A. V. Marenich, J. Bloino, B. G. Janesko, R. Gomperts, B. Mennucci, H. P. Hratchian, J. V. Ortiz, A. F. Izmaylov, J. L. Sonnenberg, D. Williams-Young, F. Ding, F. Lippa-rini, F. Egidi, J. Goings, B. Peng, A. Petrone, T. Henderson, D. Ranasinghe, V. G. Zakrzewski, J. Gao, N. Rega, G. Zheng, W. Liang, M. Hada, M. Ehara, K. Toyota, R. Fukuda, J. Hasegawa, M. Ishida, T. Nakajima, Y. Honda, O. Kitao, H. Nakai, T. Vreven, K. Throssell, J. A. Montgomery Jr., J. E. Peralta, F. Ogli-aro, M. J. Bearpark, J. J. Heyd, E. N. Brothers, K. N. Kudin, V. N. Staroverov, T. A. Keith, R. Kobayashi, J. Normand, K. Raghavachari, A. P. Rendell, J. C. Burant, S. S. Iyengar, J. To-masi, M. Cossi, J. M. Millam, M. Klene, C. Adamo, R. Cammi, J. W. Ochterski, R. L. Martin, K. Morokuma, O. Farkas, J. B. For-esman and D. J. Fox, *Gaussian 16 Rev. C.01*, Gaussian Inc., Wallingford, CT, 2016.

24 A. G. Starikov, R. M. Minyaev and V. I. Minkin, Mechanisms of Inversion of Bond Configuration at the Tetrahedral Boron Atom in Five-Membered Chelate Cycles, *Russ. Chem. Bull.*, 1999, **48**, 250–255.